JOURNAL OF GEOPHYSICAL RESEARCH, VOL. 106, NO. B5, PAGES 8871–8886, MAY 10, 2001

New gravity data in the Arctic Ocean: Comparison of airborne and ERS gravity

Vicki A. Childers,[1] David C. McAdoo,[2] John M. Brozena,[1] and Seymour W. Laxon[3]

Abstract. New gravity fields from airborne gravimetry and from ERS-1 and -2 satellite altimetry cover extensive portions of the Arctic Ocean. These two data sets may constitute as much as 60% of the data contributions to the Arctic Gravity Project compilation. Here we evaluate the accuracy and resolution of these data and quantify their impact on the compilation. Both gravity determinations compare favorably with Geological Survey of Canada surface measurements in the Beaufort Sea (airborne, 1.86–2.09 mGal rms; ERS, 2.64–3.11 mGal rms). Comparisons between the airborne and ERS data over the Chukchi Borderlands reveal a 4.38 mGal rms difference over the smoother region of the field and 7.36 mGal rms over the rugose field generated by the shallow ridges and deep troughs. Coherency between the two data sets in the Chukchi region implies a resolution of 19 km. Comparison with Science Ice Expedition submarine measurements over Chukchi Plateau suggests that the ERS field resolves even shorter-wavelength signal than the airborne data, whereas in the Beaufort Sea the airborne data showed better coherence to ground truth data. Long-wavelength differences exist between the two data sets, expressed as a 2–3 mGal offset over the Chukchi region. This study highlights the respective strengths of the two data sets. The ERS gravity field has the advantage of ubiquitous coverage of the ocean south of 81.5°N, a denser sampling of the gravity field, and a recovery of signal down to ~15 km. The airborne data cover a significant portion of the polar hole in the satellite coverage, have lower measurement noise, and recover somewhat higher anomaly amplitudes in the 25–100 km wavelength range.

1. Introduction

The origin and evolution of the Arctic Ocean are two of the largest remaining uncertainties in plate tectonics. Whereas the opening histories of the world's other major ocean basins have been understood for more than 20 years, the formation of the Arctic's Amerasia Basin remains a mystery. To date, the primary impediment to a fuller tectonic understanding has been the dearth of available geophysical data in the Arctic Ocean. Logistical problems, due to the year-round ice cover, were compounded by Cold War political sensitivities; as a result, the ocean basin was poorly sampled with bathymetry, gravity, and magnetics data. Moreover, much of the data actually collected was classified.

The past decade has seen a dramatic increase in the collection of new geophysical data in the Arctic. Large portions of the Arctic Ocean gravity field have now been mapped using two completely different techniques for determining the gravity field. The U.S. Naval Research Laboratory (NRL) has conducted an aerogeophysical campaign covering nearly 3×10^6 km^2 in the Arctic Ocean. New techniques for processing the European Space Agency's Earth Remote Sensing (ERS) -1 and -2 satellite altimeter data have yielded the first detailed gravity field over the ice-covered regions of the Arctic Ocean from satellite data [*Laxon and McAdoo*, 1994, 1998]. These two data sets overlap over much of the ocean basin. Each extends into regions unmapped by the other. In light of the recent Arctic Gravity Project (ArcGP) compilation effort spearheaded by the International Association of Geodesy (IAG) and the National Imagery and Mapping Agency (NIMA) [*Forsberg and Kenyon*, 1999], of which these two data sets will constitute a significant contribution, it is important to understand how these data sets compare in terms of accuracy and resolution. This study compares these two data sets over two regions of overlap in the Amerasia Basin. First, both sets are compared separately with high-quality ice surface gravity measurements in the Beaufort Sea region (Figure 1) of the Canada Basin, and then with each other and with Science Ice Expedition (SCICEX) submarine gravity measurements over the rugose gravity field of the Chukchi Borderland.

2. Geologic Context

In the Arctic Ocean the Amerasia Basin extends southward from the Lomonosov Ridge toward the continental margins of Canada, Alaska, and Siberia. The southernmost portion of the Amerasia Basin covered in this study includes the Canada Basin, the Chukchi Borderland, and the Northwind Ridge (Figure 1).

The Canada Basin extends from the Canadian and Alaskan continental margins westward to the Northwind Ridge and Chukchi Borderland. The Alpha and Mendeleev Ridges define the northern limits of the basin. Water depths exceed 3 km throughout most of the basin and reach a uniform depth of

[1]Naval Research Laboratory, Washington, D.C.
[2]Laboratory for Satellite Altimetry, NOAA, Silver Spring, Maryland.
[3]Mullard Space Science Laboratory, University College London, Dorking, England, United Kingdom.

Paper number 2000JB900405.
0148-0227/01/2000JB900405$09.00

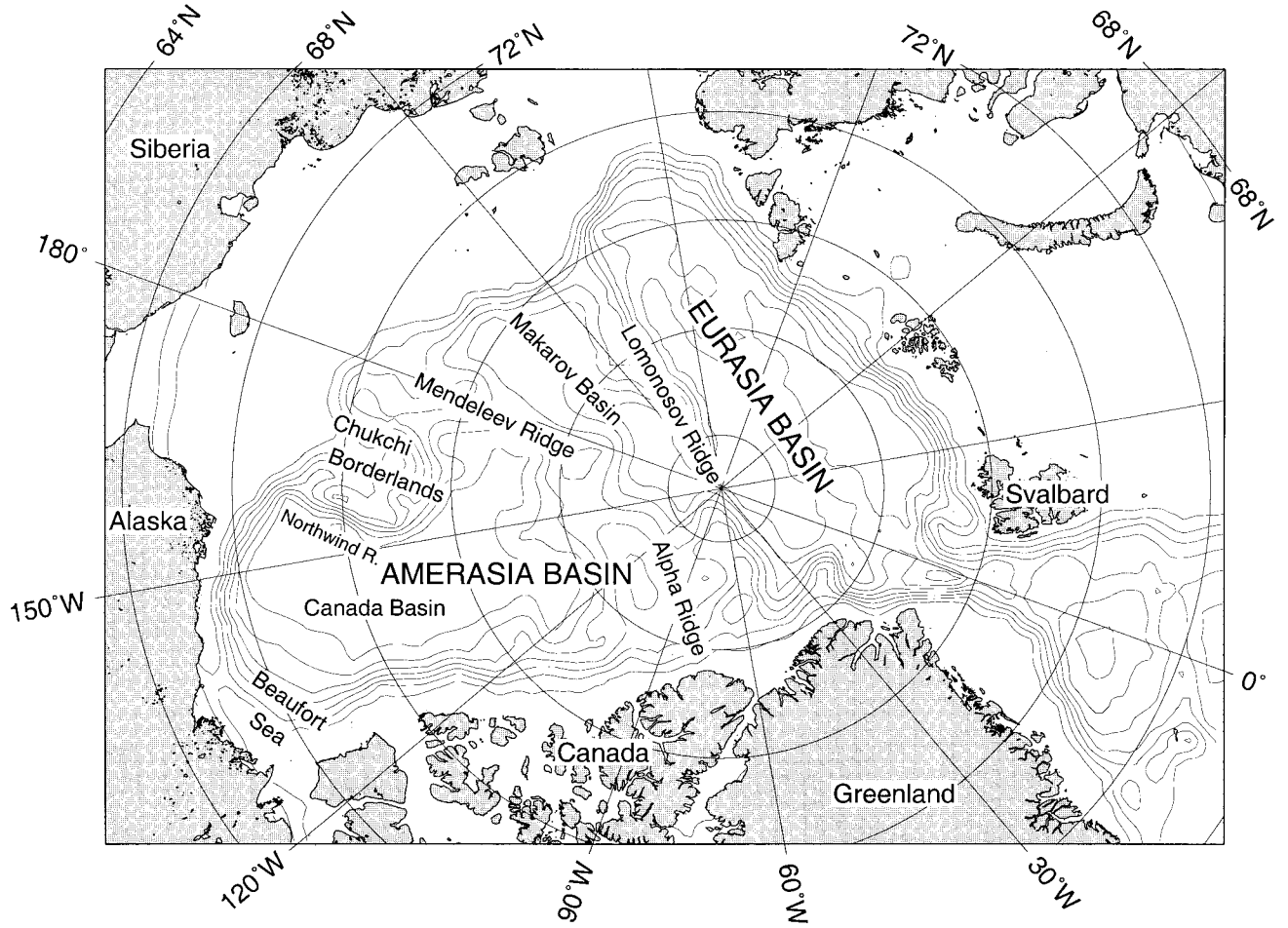

Figure 1. Map of the Arctic Ocean denoting physiographic features. The first contour line offshore denotes 500 m; the remaining lines indicate 1000-m intervals.

3850 m in the Canada Abyssal Plain, located along the western third of the basin [*Johnson et al*., 1990]. Estimates of sediment thickness range from 12 km near the southeastern margin to 6 km in the abyssal plain [*Grantz et al*., 1990].

Extending northward from the Canadian margin in the center of the basin is a long linear gravity low with flanking highs [*Laxon and McAdoo*, 1994] that is not expressed in the bathymetry [*Vogt et al*., 1982]. This feature trends northward from the Mackenzie Delta and approximately bisects the Canada Basin; it has been proposed as an extinct spreading center based upon its anomaly shape and location [*Laxon and McAdoo*, 1994]. The spreading center identification of this feature is consistent with a suite of models for the formation of the Canada Basin that favor a rotational, fan-shaped opening of the basin (see review by *Lawver and Scotese* [1990]). Rotational models suggest that the Arctic Canada, Alaska, and Siberian margins are passive. Other workers [*Lane*, 1997] disagree with the rotational models and the interpretation of the linear low as an extinct spreading center. They propose that the basin opened in a north-south direction which implies that one or more of the above mentioned margins is a strike-slip plate boundary [*Lane*, 1997] (see review by *Lawver and Scotese* [1990]). We favor the extinct spreading center interpretation based upon the morphology of the ridge, and the symmetric magnetic anomalies either side of the ridge axis that resemble seafloor spreading anomalies [*Brozena et al*., 1999; *Taylor et al*., 1981].

The Chukchi Borderland is a complex region located just basinward of the Siberian margin in the Canada Basin that includes at least three approximately north-south trending segmented ridges separated by abyssal plains. The ridges, which include the Northwind Ridge, the Chukchi Cap and Rise, have steep flanks and plateau-like crests that stand as much as 3400 m above the surrounding seafloor, while the intervening abyssal plains lie at depths of 2100 to 3850 m [*Hall*, 1990]. The most dramatic of these ridges is the Northwind Ridge, which forms the eastern boundary of the borderland.

While it is generally agreed that the Chukchi Borderland is composed of continental crustal fragments rifted off of a continental shelf because of the ridge elevations and their low-amplitude magnetic signature [*Taylor et al*., 1981; *Vogt et al*., 1981], there is disagreement as to its original location. Various models of Canada Basin formation involve the Chukchi Borderland being originally part of the Siberian shelf, the Alaskan shelf, and the Canadian shelf (see review by *Hall* [1990]). Permian red bed sediments and other rocks recently dredged from Northwind Ridge demonstrate an affinity with Triassic and older rocks of the Sverdrup Basin of the Canadian Arctic Archipelago [*Grantz et al*., 1998], supporting the theory of the

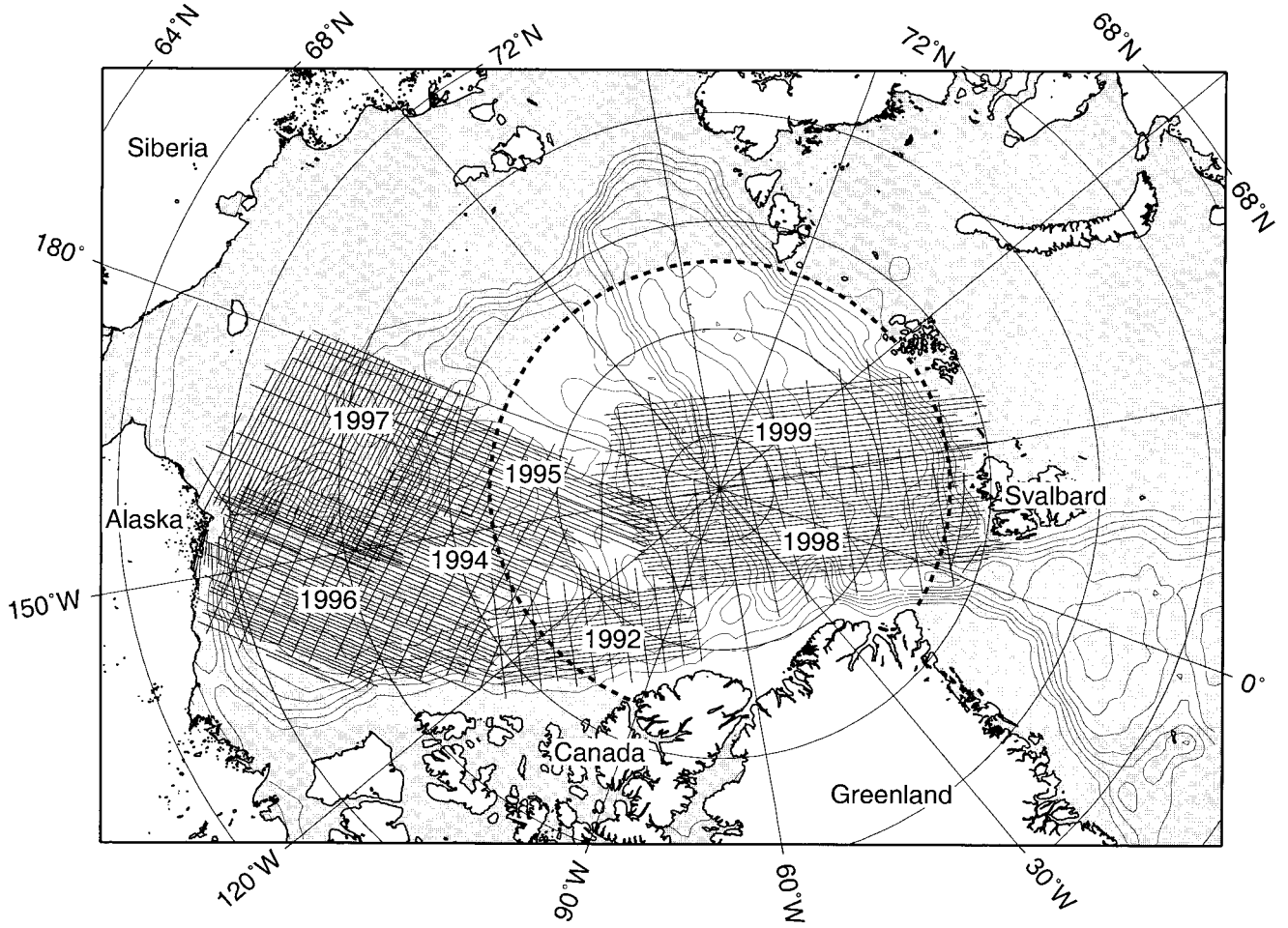

Figure 2. Coverage of the NRL airborne surveys and the ERS 1998 gravity field. The shaded ocean region denotes ERS 1998 coverage, with the dashed line indicating the northernmost extent. The survey lines with year labels denote the various airborne field seasons.

Borderland's original attachment to Arctic Canada and Alaska prior to rifting.

3. New Arctic Gravity Data

The new NRL airborne gravity and the ERS altimetric gravity data sets cover extensive regions of the Arctic Ocean (Figure 2). The ERS gravity field provides continuous marine coverage south of 81.5°N, and denser, more uniform sampling than the NRL survey. In addition, the ERS-1 and -2 satellites have collected a tremendous amount of data in their 8 years of operation. The NRL aerogeophysics program, on the other hand, has surveyed a large portion of the deep water Arctic including about half of the region north of 81.5°N. This comparison provides a unique opportunity to evaluate both data sets.

3.1. NRL Aerogravimetry

Airborne gravimetry has the unique ability to recover an accurate gravity field over any continent, coastal area, or ocean within range of aircraft operations. The range of the NRL survey capability is maximized through use of the U.S. Navy P-3 Orion aircraft. Designed for submarine surveillance, the P-3 can cover up to 6000 km in a single flight at 250 knots at altitudes of 600 m or less. In the Arctic, airborne surveying has proven to be an effective method for collecting gravity and other geophysical data. NRL has now completed seven field seasons in the Arctic, measuring gravity and magnetics along 210,000 line km, covering nearly two thirds of the Arctic Ocean basins (Figure 2). In addition, a host of smaller-scale, higher-resolution airborne surveys have been conducted in the Arctic, using smaller twin engine aircraft, by Danish, Norwegian, German, and Canadian researchers [*Forsberg et al*., 1999; *Forsyth et al*., 1994; *Timmen et al*., 1998].

The goal of the NRL aerogeophysics program is to provide continuous measurement of gravity and magnetics across the Arctic Ocean to help clarify the structure and tectonic evolution of the region. Airborne data used in this study were collected in collaboration with the University of Texas Institute for Geophysics during the 1996 and 1997 field seasons, covering the Beaufort Sea and the Chukchi Borderland. Survey design and flight characteristics for the two surveys are listed in Table 1. Data from all seven NRL Arctic surveys will be integrated into the ArcGP compilation and the data from these two surveys will be released separately after publication of Canada Basin research.

The P-3 aircraft is equipped with two LaCoste and Romberg marine gravimeters modified for airborne use. Postmission positioning is calculated from GPS carrier phase data collected

Table 1. Survey Design and Data Parameters for the 1996 and 1997 NRL Arctic Field Seasons[a]

Year	Base Airport	Speed, knots (km/h)	Altitude, m	Data Line, km	Cross Track, km	Filter Half-Amplitude Point 5 (km)	Crossover, mGal rms
1996	Barrow, Alaska	265 (491)	783	11–15	50	250 (34)	2.0
1997	Barrow, Alaska	259 (479)	535	11–18	70	167 (22)	1.8

[a]Values of aircraft speed and altitude are averaged for the surveys. Dataline and cross-track spacing and filter half-amplitude point impact data resolution. The final column displays rms mistie at intersections. In 1997, the 11-km line spacing was used over the Northwind Ridge to preserve higher-frequency information.

simultaneously by Ashtech Z-12 dual-frequency receivers in the aircraft and at a base station using the XOMNI software [*Ball et al*., 1995]. Aircraft attitude information is supplied by a Litton 72 inertial navigation system. A radar altimeter provides additional aircraft altitude and vertical acceleration information.

Isolation of the gravity signal from the effects of aircraft motion is the primary challenge in airborne gravimetry. The aircraft acceleration measured along the local vertical by the gravimeters is differenced with the vertical acceleration of the aircraft, usually determined from the GPS altitudes. The resultant accelerations are corrected with the Eötvös, latitude correction, and free-air corrections to yield the free-air anomaly at aircraft altitude [*Harlan*, 1968; e.g., *Telford et al*., 1990]. The use of radar altitudes for the free-air correction references the free-air anomaly to the geoid. The free-air anomaly is further corrected for offleveling errors that result when horizontal accelerations from aircraft trajectory drive the gyrostabilized gravimeter platform offlevel [*Peters and Brozena*, 1995]. Final noise reduction in the free-air anomaly is achieved through a cosine taper low-pass filter applied in the frequency domain. This filter is tailored to best remove noise while optimizing the signal based upon aircraft speed and altitude and noise characteristics of the survey [*Childers et al*., 1999]. The free-air anomalies generated from each gravity meter are then averaged. Next, a least squares network adjustment is applied to the survey to minimize intersection differences [*Peters and Brozena*, 1988]. Filtering parameters and rms intersection differences for the two surveys are listed in Table 1.

Signal loss in the free-air anomaly results from measurement noise and upward continuation error from measurement at altitude. Low-pass filtering, required to minimize measurement noise, and upward continuation both attenuate shorter-wavelength anomalies. Errors remaining after filtering in the gravimeter measurement are generally related to aircraft motion, whereas GPS errors scale with baseline distance and levels of ionospheric disturbance. Measurement error in both the gravimeter and GPS systems tend to be expressed as oscillatory errors of a few milliGalls superimposed upon the gravity signal. Overall error in the seven surveys as expressed by intersection differences ranges from 1.8 to 3.5 mGal rms, with the Chukchi Borderland survey at 1.8 mGal.

Although the resolution is explicitly defined by the signal-to-noise ratio, the effective resolution of the airborne data in the along-track direction is constrained primarily by the low-pass filter. The measurement noise is "blue" in character, with amplitude that is small at the longest wavelengths but increases quickly with decreasing wavelength. The filter that optimizes signal recovery for a given survey determines the remaining spectral content. Filtering for the Beaufort Sea survey reaches half amplitude at 250 s (34 km full wavelength) and for the Chukchi Borderland survey reaches half amplitude at 167 s (22 km). Cross-track resolution is twice the data line spacing and is enhanced near cross tracks. Average resolution along/across track is 34/28 km for the Beaufort Sea survey and 22/30 km for the Chukchi Borderland. In general, for gridded surveys the data are aliased in the cross-track direction. The block mean function in the generic mapping tools (GMT) [*Smith and Wessel*, 1990] software is used to average data within a grid cell to reduce aliasing effects. Size of the grid cell is selected to improve aliasing without adding too much extra filtering.

3.2. ERS Satellite Gravity

One of the most exciting developments in marine geophysics has been the determination of the global marine gravity field from satellite altimetry. Because the mean topography of the sea surface approximately conforms to the geoid and reflects variations in the Earth's gravity field, the ocean surface can be differentiated to yield an estimate of the gravity field. These estimates neglect the effects of ocean dynamics which are thought to be small in the Arctic. Over ice-free oceans, radar altimeter data from the ERS-1 and Geosat satellites have been used with great success to determine the Scripps/NOAA global marine gravity fields up to 72° latitude [*Andersen and Knudsen*, 1998; *Sandwell and Smith*, 1997]. ERS-1 (1991 to 1996) and its successor satellite ERS-2 (1995 to present) operate from a higher-inclination (82°) orbit than Geosat and Seasat and therefore observe the sea surface farther north, i.e., up to 82° latitude. However, over most of the Arctic Ocean standard ERS altimetric "ocean data products" (OPRs) from the altimeter trackers onboard the ERS satellites cannot be used because the highly specular radar echoes from sea ice confuse the onboard data processor. Nevertheless, as *Laxon and McAdoo* [1994, 1997] showed, a laborious analysis of the full ERS waveform product (WAP) data set (much larger than the OPR data set) can be used to recover accurate estimates of sea surface topography and therefore, gravity, over the largely ice-covered circum-Arctic Ocean, thereby extending existing altimetric gravity fields of the global ocean [*Sandwell and Smith*, 1997] north to 82° latitude. This analysis of the ERS waveforms mitigates contamination (e.g., via pulse blurring) of the surface topographic signal by sea ice [*Laxon*, 1994].

Suitable waveforms (WAPs) are reprocessed using a simple threshold-retracking algorithm to recover acceptable estimates of sea surface height and thence along-track slope, or deflection of the vertical. The long-wavelength (>2000 km) component of the field is first removed using the JGM-3S [*Nerem*, 1994; *Tapley et al*., 1996] satellite tracking field. Using splines in tension [*Smith and Wessel*, 1990], the ascending and descending slopes are independently interpolated onto a grid with intervals of 0.025° latitude and 0.10° longitude (~2.5 km × 2.5 km grid). Ascending and descending slopes are resolved into

north and east components and are used to generate a conventional deflection of the vertical vector field. Using an inverse Vening-Meinesz transformation via a fast Fourier transform (FFT) algorithm, the marine gravity field is generated from this deflection of the vertical field. Afterward, the long-wavelength field that was previously removed is restored [*Laxon and McAdoo*, 1997; *McAdoo and Marks*, 1992].

With the shutdown of ERS-1 in 1996, an improved Arctic Ocean gravity field (1997, 1998) was derived using all available ERS-1 data including the geodetic phase data. (This ERS-1-only field is available on the web at http://ibis.grdl.noaa.gov/SAT or http://wwwcpg.mssl.ucl.ac.uk/people/swl/.) *Laxon and McAdoo* [1994, 1998] have continued to significantly improve the ERS Arctic Ocean gravity field by incorporating the many new repeat cycles of altimeter (WAP) data from the ERS-2 satellite. ERS-2 was launched in 1995 and continues to observe along the same 35-day ground track begun by ERS-1. By incorporating these additional ERS-2 WAP data into the gravity estimation one continues to reduce measurement noise from sea ice and other sources. (The first of these new fields, ERS 97W, is now available on the web at http://wwwcpg.mssl.ucl.ac.uk/people/swl/.) The ERS-1 and -2 marine gravity used in this paper is an interim field computed for the Canada Basin region of the Arctic using the ERS-1 data plus nine 35-day cycles of ERS-2 data. This field, herein after referred to as the ERS 1998 field, was presented at the International Conference on Arctic Margins (ICAM) III in Celle, Germany, October 1998. Further improvements have been realized via refinements in waveform processing and gravity estimation techniques. The ERS 1998 field is an incremental improvement over the ERS 1997-W (Web data set) field and will be incorporated into a new ERS field anticipated for release in 2001.

Among the significant recent improvements in gravity estimation techniques is the inclusion of detailed land gravity in near-coastal land areas adjacent to the Arctic Ocean in our computations of ERS gravity. Over areas such as parts of northern Alaska or Siberia, where point data were unavailable, NIMA 30-min mean free-air anomalies [*Lemoine et al*., 1998] were used. The following steps were taken: (1) land data were gridded, low-cut filtered by removing a rolled-off JGM-3S background field; (2) the resulting gravity grid was converted to a grid of deflections of the vertical by using FFT techniques to accomplish the forward Vening-Meinesz transformation; (3) these deflections of vertical were converted to pseudo, overland, along-track slopes using ERS ground track geometry; and (4) the pseudoslopes were concatenated with the actual marine ERS data during the gridding of ascending and descending ERS slope data. Thus the detailed land gravity data were included as far-field input in our inverse computations of marine gravity data. As a result, the accuracy of the ERS Arctic gravity field in coastal waters was significantly improved over that of earlier ERS fields [*Laxon and McAdoo*, 1994, 1997].

Aside from the sea ice challenge, ERS-1 and -2 data possess several unique advantages for determination of the Arctic marine gravity field. The close satellite track spacing at high latitudes (~2 km at 75°N) provides denser data coverage than at lower latitudes. Also, the sea state, a limiting factor in the resolution of the technique in open water, is less a factor in the Arctic where the sea ice attenuates the surface wave action. Resolution in the ERS data set, as with all pulse-limited radar satellite altimeters, is limited by the area of the sea surface sampled by the radar's effective "footprint." The footprint of the ERS-1 and -2 altimeters is at least several kilometers across. Such distributed observations of height, as opposed to point observations, make resolution of short-wavelength (<15 km) gravity signals nearly impossible.

Resolution limits on airborne gravimetry (from filtering) and on the satellite gravity field (from radar footprint) are similar in magnitude. Thus a comparison between the overlapping surveys is necessary to understand differences in resolution and accuracy, their implications for tectonic interpretation, and the combining of these data sets in the ArcGP compilation.

4. Data Comparison in the Amerasia Basin

4.1. Comparison Methodology

The data sets involved in this study vary significantly in spatial distribution of measurements. The airborne data were measured along a survey grid and the ERS 1998 gravity field is distributed evenly in latitude and longitude. The surface gravity data vary in distribution including both point measurements and shipboard survey profiles.

To aid in the statistical comparison of data sets with differing spatial distributions, we used two techniques. First, we interpolated ERS 1998 data and the surface data using splines in tension [*Smith and Wessel*, 1990]. Both interpolated data sets were sampled at each point along the airborne track to yield profile representations for time series analysis. For each track the data sets were compared using rms and mean differences along the profile. As an independent estimate of the rms and mean differences, the original data sets were also compared by evaluating "nearest-neighbor" points: a point in one set that is located within 1 km of a data point in another. This method avoids the introduction of any error through additional interpolation and provides a population-based estimate of the comparison statistics over a broad region.

For spectral analysis, data along all profiles were sampled at 0.1 km and were trimmed to contain the same number of points while maximizing the similarity between the profiles through selective cutting. Spectral estimates of power and coherence were calculated using *Welch*'s [1967] method of averaging over modified periodograms. A transform window width of 2048 points, or 204.8 km, provided five overlapping transforms per profile. Because of the similarity of the gravity field over the region covered by the tracks selected, for a given data type each profile was considered to be an independent realization of the same process. This way the long transform window could be used to preserve detail in the long wavelengths while reducing the variance to acceptable levels by averaging the estimates of all the profiles.

4.2. Beaufort Sea Comparison

In the Beaufort Sea in the southern Canada Basin, both the airborne and the ERS gravity data sets overlap ice surface and shipboard gravity measurements taken along the Arctic Canada and Alaska margins (Figure 3). The Geological Survey of Canada (GSC) made high-quality ice surface gravity measurements starting at the Canadian coastline and extending past the shelf break into the ocean basin [*Sobczak et al*., 1990]. These data consist of land meter measurements taken on the ice surface every 3–10 km with an average spacing in the region of comparison of ~5 km (Figure 3). Along the Arctic Alaska margin, shipboard gravity surveys were compiled by the U.S. Geological Survey (USGS). These data are of lesser quality for

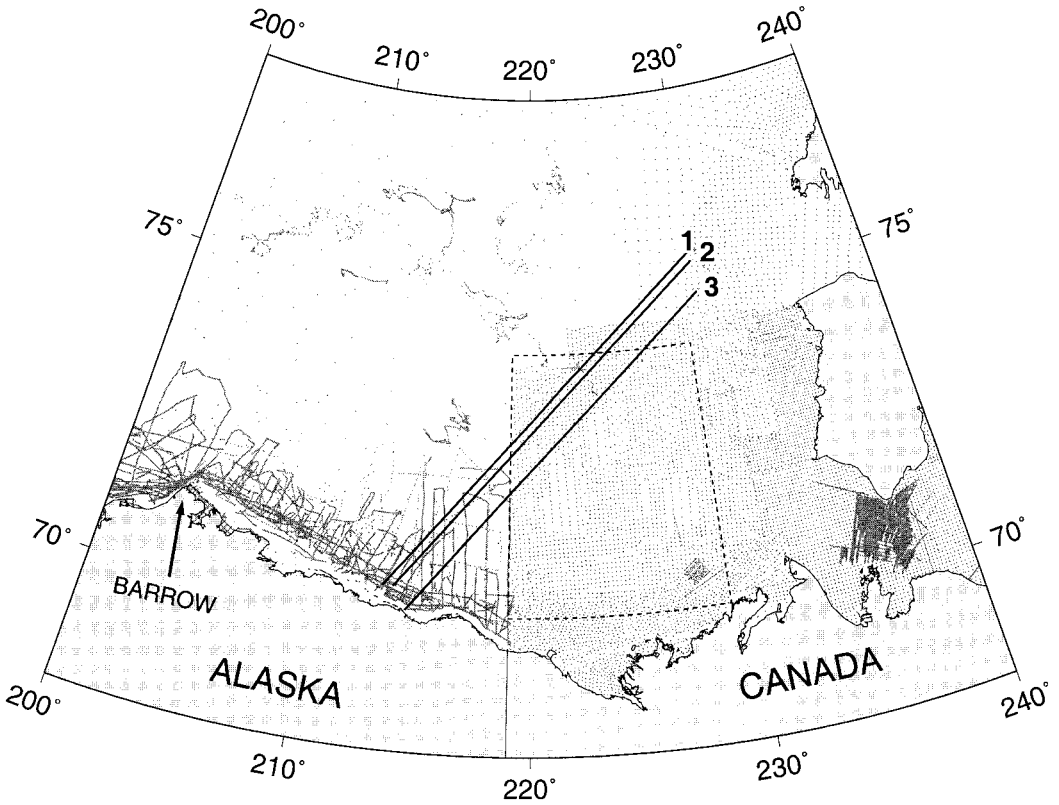

Figure 3. The Beaufort Sea region with the Geological Survey of Canada (GSC) ice surface and U.S. Geological Survey (USGS) shipboard gravity data locations shown as shaded. The airborne profiles are lines 1, 2, and 3, and the dashed box denotes the region used for the ERS 1998/GSC data comparison.

constructing a "ground truth" test field because the survey lines are widely spaced and some have erroneous ties. Thus our comparison focuses on overlap with the higher-quality GSC data set.

Three airborne profiles from the 1996 survey were selected that overlap with the surface data (Figure 3). Airborne and sampled ERS 1998 profiles are compared with sampled profiles of the GSC/USGS data (Figure 4), and the rms and mean differences are calculated with respect to the GSC data (see Table 2). On average, the rms difference between the airborne data and the GSC data (1.86 mGal) is lower than the rms difference between the ERS 1998 and the GSC data (2.64 mGal). Averaged rms differences between the airborne and the ERS 1998 field is 2.55 mGal.

Visual inspection reveals the similarity between ERS 1998 and the GSC data in the Beaufort Sea region (Plate 1). As a further test, we conducted a nearest-neighbor comparison between the ERS 1998 and the GSC data over a region of the densest sampled on-ice data (see box in Figure 3 and Plate 1) and between the airborne data and any overlap with the GSC data (Figure 3). Nearest-neighbor analysis yields a similar result to the profile comparison with airborne minus GSC at 2.09 mGal and ERS 1998 minus GSC at 3.11 mGal rms.

For spectral analysis the entire profiles were used to provide a better spectral estimate. Power spectral density estimates indicate similar power levels in all three data sets at wavelengths of 60 km and longer (Figure 5). The power in the airborne signal is equivalent to the surface data at wavelengths of 40 km and longer and then begins rolling off in response to the low-pass filter used in the final processing. The coherence between the airborne and the surface data drops to 0.5 at 28 km, close to the 32.5 km half-amplitude point of the low-pass filter employed for this airborne survey. The power in ERS 1998 is somewhat lower than the surface and airborne data in the 50–35 km wavelengths and matches the surface data again at wavelengths in the 30–22 km range. Coherence of ERS 1998 with the surface data drops to 0.5 at ~39 km.

4.3. Chukchi Borderland Comparison

We extend the comparison between the airborne data and ERS 1998 to the Chukchi Borderlands. The 1997 airborne survey covers the Chukchi ridges and troughs and the Siberian continental shelf just west of the ridges. ERS 1998 covers the entire airborne survey (Plate 2). The rugose character of the field provides an interesting opportunity for comparison between the two gravity determinations even though there are no ground truth data available for comparison.

Five airborne tracks were selected over a region of high-amplitude, short-wavelength gravity anomalies for profile comparisons (Figure 6). ERS 1998 minus airborne comparisons yield an mean rms difference of 7.48 mGal (see Table 3). Visual inspection of the profiles reveals that the largest differences exist over the high-amplitude, short-wavelength anomalies.

The nearest neighbor analysis of the region shown in Plate 2 yields 6689 data points between the two data sets that are located within 1 km of each other. The rms difference of this estimate (6.02 mGal) is somewhat less than the profile comparison, reflecting an average measure of the entire region.

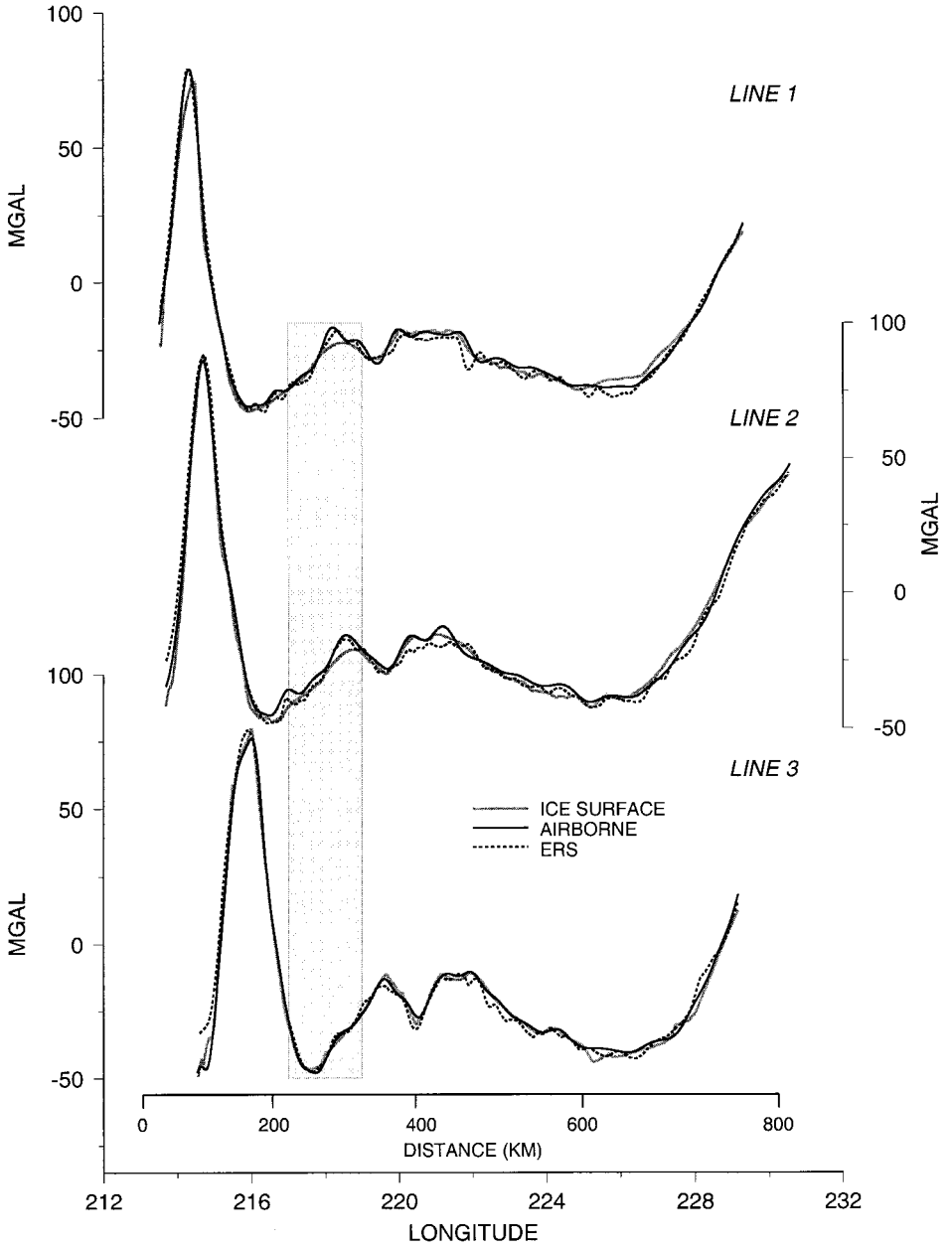

Figure 4. Three airborne profiles over the Beaufort Sea region located in Figure 3. The solid line represents the airborne measurement, the dashed line represents the ERS 1998 field, and the shaded line represents the sampled GSC/USGS data. Gray box denotes a region of minimal surface data.

Plotting these nearest-neighbor differences as a function of longitude (Figure 7) shows that the preponderance of large differences occur over the region east of 193.65°E, where the ridges and troughs of Chukchi Borderland create a high-gradient, high-amplitude field with significant power in the shorter wavelengths. For the population of differences east of the 193.65°E meridian the rms difference is 7.36 mGal, while west of the meridian the rms difference is 4.38 mGal. The mean difference between the data sets also varies either side of this meridian: east is 2.17 mGal, west is 2.77 mGal.

Spectral analysis of the profile data (Figure 5) suggests that less power exists in ERS 1998 than in the airborne signal at wavelengths >22 km. At wavelengths <22 km, power drops off quickly for the airborne data as a result of the low-pass filter; however, power still remains in the ERS signal at shorter

Table 2. Comparisons Between Both the Airborne and ERS-1 and -2 Gravity Field With the GSC Surface Data in the Beaufort Sea[a]

	Airborne Minus GSC		ERS Minus GSC	
Track	Mean, mGal	rms, mGal	Mean, mGal	rms, mGal
1	−0.22	1.85	−1.42	2.76
2	0.51	2.05	−1.38	2.58
3	0.72	1.68	−0.22	2.57
Track average	0.34	1.86	−1.01	2.64
Nearest neighbor	0.56 (n = 146)	2.09	0.78 (n = 821)	3.11

[a]Statistics are shown for each track and then averaged for all tracks. Comparison between "nearest neighbors" is given: a point in one data set located within 1 km of a point in the other; n is the sample size.

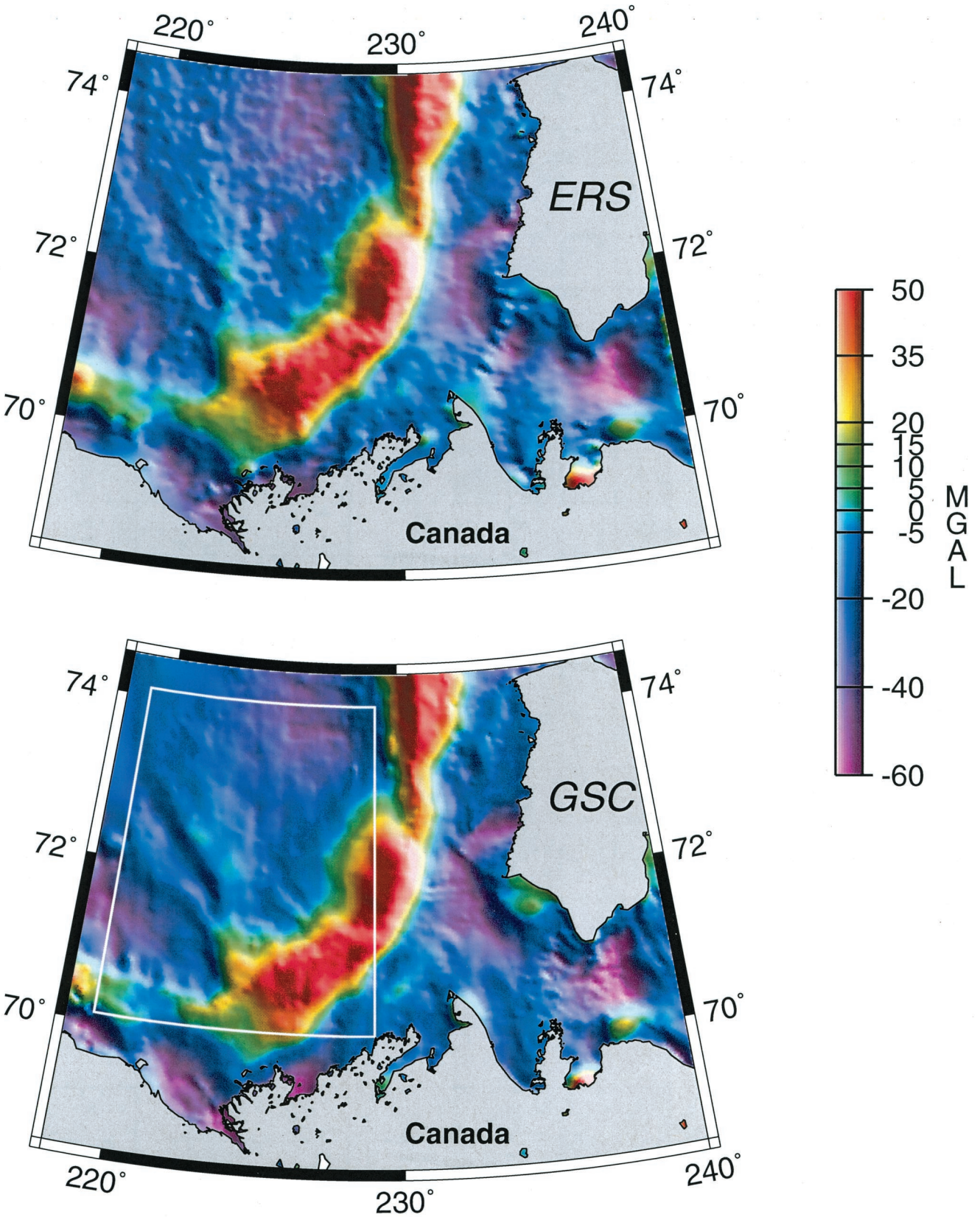

Plate 1. ERS 1998 and GSC ice surface data gridded in the Beaufort Sea. The box outlined in white denotes the region of comparison of the two gravity determinations.

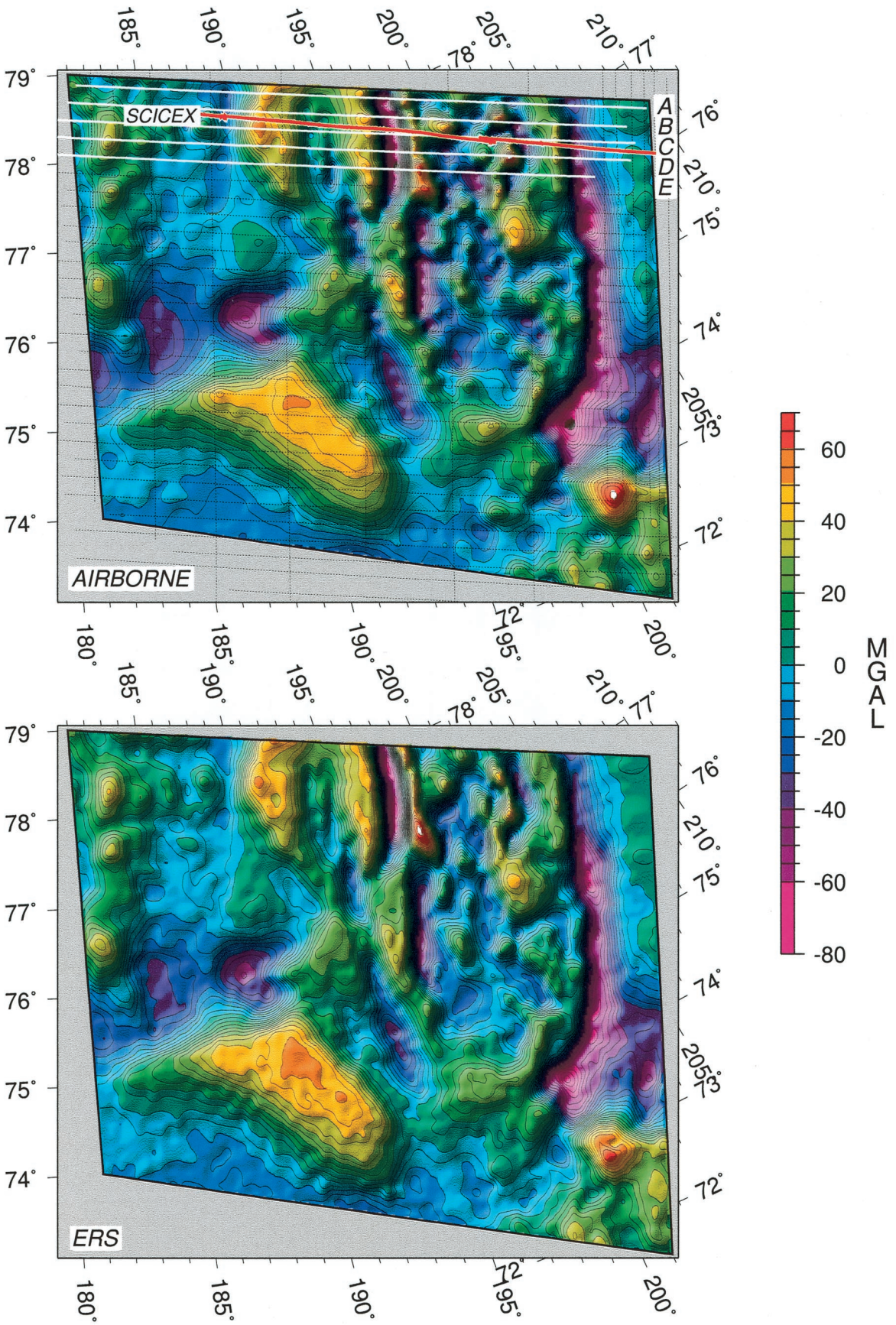

Plate 2. Gridded airborne data and ERS 1998 over the Chukchi Borderland. Dotted lines denote airborne tracks, white lines locate the profiles compared in Figure 6, and the red line shows the location of the SCICEX 1995 USS *Cavalla* submarine track.

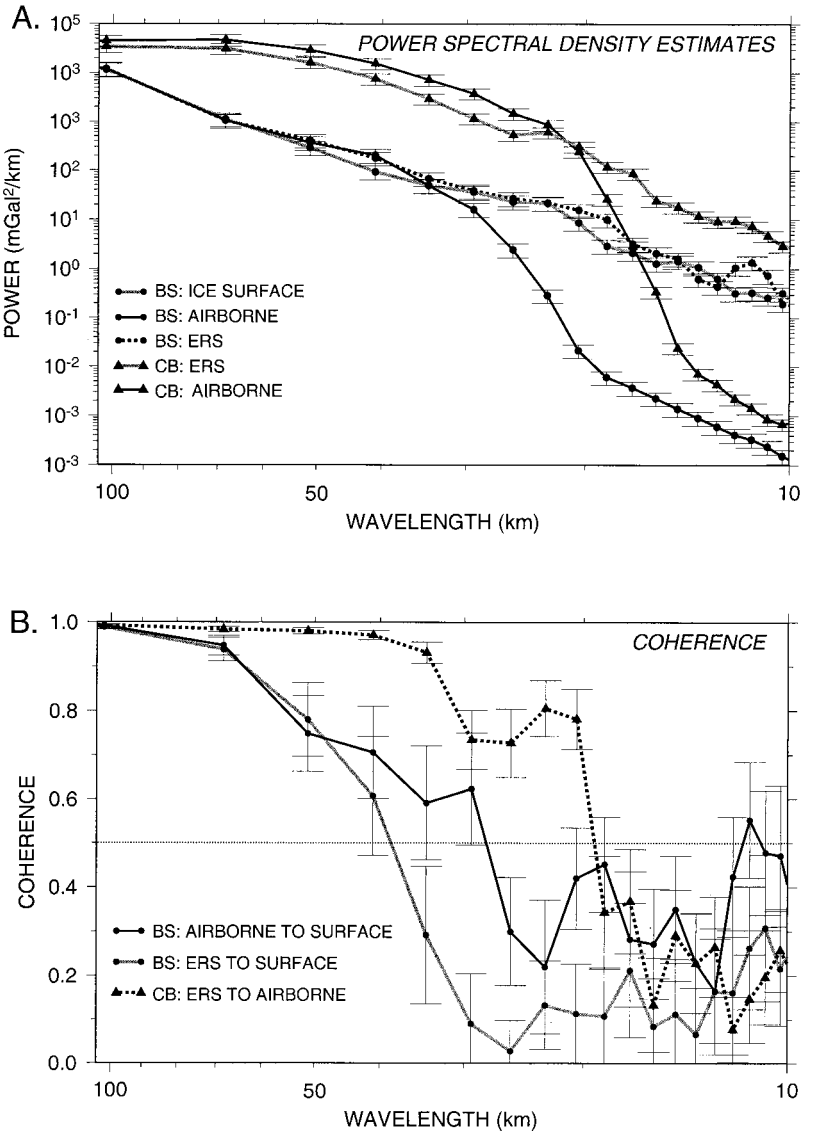

Figure 5. Spectral estimates of (a) power and (b) coherence of the profile data. Circles indicate estimates for Beaufort Sea comparison, and triangles indicate estimates for Chukchi Borderland comparison.

wavelengths. Coherence between the two signals drops to 0.5 at 19 km.

An additional data comparison over the Chukchi Borderland is possible with gravity measurements made aboard the USS *Cavalla* submarine as part of the 1995 SCICEX program [*Pyle et al*., 1997]. One submarine survey line crosses the Chukchi Plateau at a slightly different heading but overlaps a portion of airborne track C over the middle of the rugose field. Airborne data along track C are shown with the submarine data and ERS 1998 sampled along the submarine profile (Figure 8). Notice the higher amplitude of the short-wavelength anomalies measured from the submarine. The steady motion of the submarine free from surface dynamics requires only 2–3 min of low-pass filtering in the data processing, and most importantly, the low-pass filter extends over a smaller spatial distance given its slower surveying speed. Moreover, measuring gravity closer to the anomalous source enhances shorter-wavelength recovery. Also of interest are small-scale features present in the submarine and ERS data that are absent in the airborne data, for example, at 198°, 200°, and 204°E. These features are lost to the airborne filtering and upward continuation effects. Coherence between ERS 1998 and the *Cavalla* data, like that between the airborne data and ERS 1998 data, drops to 0.5 at 19 km.

Of interest in the comparison between the data sets over Chukchi Borderland is a difference of mean levels not seen in the Beaufort Sea area. The nearest-neighbor analysis suggests a varying of mean level difference east and west of 193.65°E. A best fit plane through the nearest-neighbor differences over the entire Chukchi survey region demonstrates a bias and a tilt to the differences, with ERS 1998 data higher than the airborne by 2.48 mGal on average. The direction of maximum increase is nearly coincident with the direction of decreasing longitude with a minimum of 1.61 mGal on the eastern edge of the region to a maximum of 3.26 mGal on the western edge. In comparison, the *Cavalla* data nearly split the difference between the other two data sets with a mean level 1.5 mGal lower than ERS 1998.

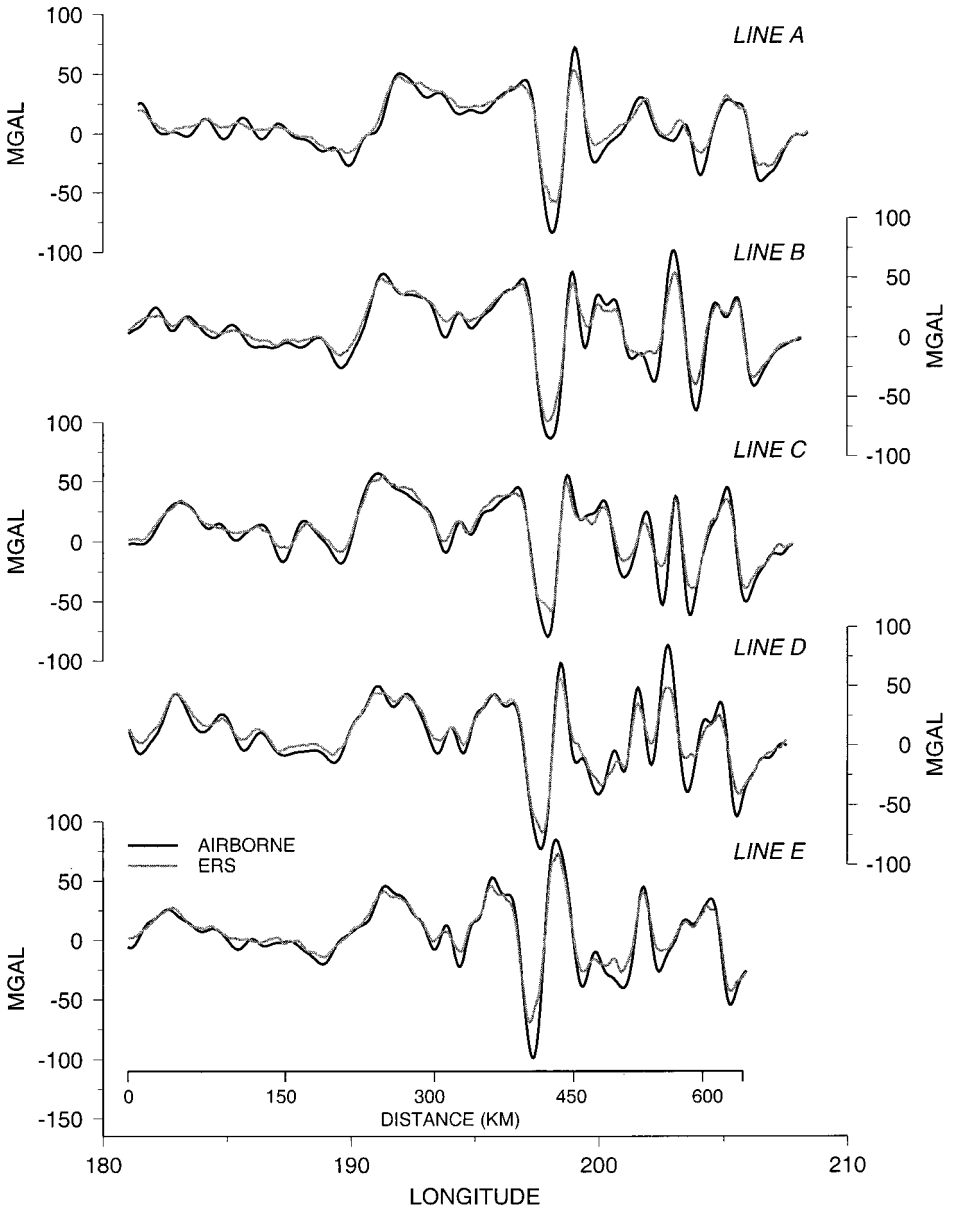

Figure 6. Airborne data and ERS 1998 sampled along the profiles shown in Plate 2. Airborne data are shown as solid curves, ERS 1998 data are shown as shaded curves.

5. Discussion

5.1. Significance of Results

Close inspection of the airborne data and the ERS 1998 field reveal their remarkable similarity. Both data sets compare well with the GSC data in the Beaufort Sea, with the airborne data having slightly lower rms differences with respect to the GSC data (~0.5–1 mGal). In the smooth region west of 193.65°E over Chukchi Borderland the rms comparison between the airborne data and ERS 1998 is 4.38–4.51 mGal, slightly higher than the comparison in the Beaufort Sea, but still quite good. It is only in the region of high-amplitude, short-wavelength anomalies over the Chukchi Borderland that there is an appreciable, systematic difference between the data sets. In this region, ERS 1998, in general, has less amplitude than the airborne data. The nearest neighbor (Figure 7) and profile comparisons (Figure 6) show the greatest differences between

Table 3. Comparison Between the Airborne and the ERS-1 and -2 Gravity Field Over the Chukchi Borderland[a]

	ERS Minus Airborne		ERS Minus Airborne (West of 193.65°E)	
Track	Mean, mGal	rms, mGal	Mean, mGal	rms, mGal
A	3.24	6.97	2.62	4.99
B	2.45	7.37	2.42	4.67
C	2.63	7.27	1.69	4.13
D	2.33	8.31	3.40	5.15
E	2.46	7.47	1.91	3.63
Track average	2.62	7.48	2.41	4.51
Nearest neighbor	2.48 (n = 6689)	6.02	2.78 (n = 3435)	4.38

[a]Statistics for each track are shown and averaged. "Nearest neighbor" compares a point in one data set that is located within 1 km of a point in the other data set for the region shown in Figure 7; n is the sample size.

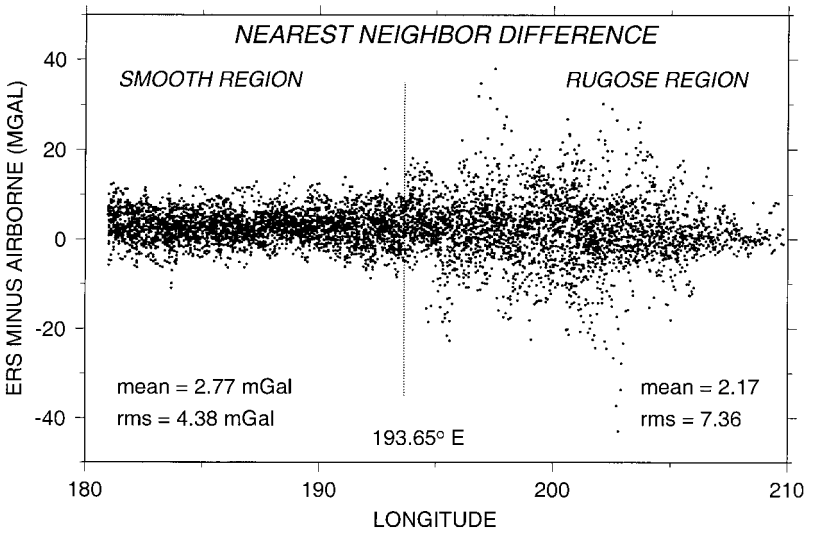

Figure 7. Comparison of 6689 points in both ERS 1998 and the airborne data located within 1 km of each other over the Chukchi Borderland. Differences are shown as ERS 1998 minus airborne. 193.65°E marks the limit of the rugose field of the Chukchi ridges and troughs. The rms and mean level difference vary between the smooth and rugose regions of the field.

the data sets exist over the rugose segment of the field. Spectral analysis of the profile data suggests that there is less power in the ERS than in the airborne data at wavelengths of 100 to 25 km, where the airborne low-pass filter begins rolling off (Figure 5). Given the low-pass filtering and upward continuation effects associated with the airborne method, the expectation would be that the airborne technique would underestimate, not overestimate, the amplitude of shorter-wavelength anomalies. Comparison with the submarine data confirms that true anomaly amplitudes exceed the airborne or the satellite determination.

Although it plays a subordinate role to low-pass filtering in attenuating anomalies, upward continuation is most significant where the source of the anomalies is shallow, as in the Chukchi

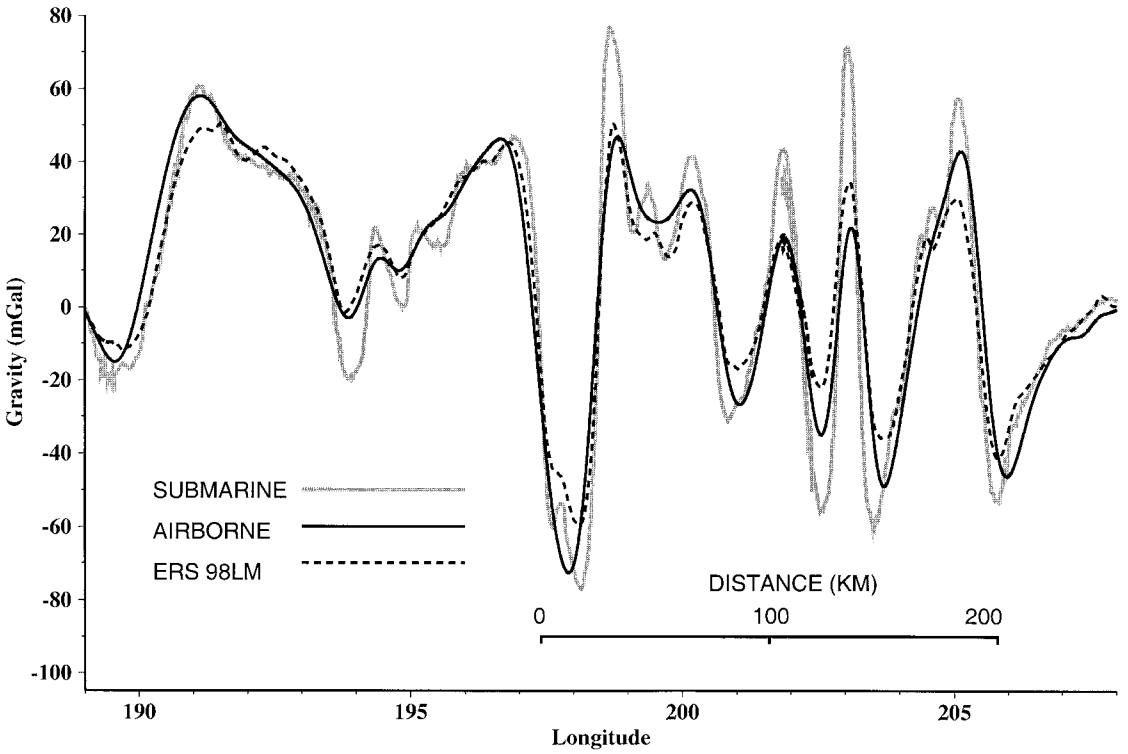

Figure 8. Gravity as measured aboard the SCICEX USS *Cavalla* submarine along the red profile in Plate 2 is shown shaded. ERS 1998 data sampled along the submarine track are shown (dashed line) as are the airborne data from nearby track C (solid line).

Borderlands. The anomaly attenuation can be calculated according to

$$y = e^{-kd}, \quad (1)$$

where y is the attenuation, k is the wavenumber (or convert to wavelength λ with $k = 2\pi/\lambda$), and d is the measurement distance [*Turcotte and Schubert*, 1982]. For the example of a long, linear anomaly with a 40-km cross-sectional wavelength at 1000 m depth (approximating a narrow ridge in the Chukchi region with a half width of 20 km), the submarine at 200 m below the surface would recover 88% of the anomaly amplitude, while an aircraft at 600 m altitude would recover 78%. However, the difference in amplitude recovery increases as the wavelength shortens: for a 20-km wavelength the recovery is 78% and 60%, respectively. For deeper water the difference in amplitude recovery between the two platforms becomes less significant. At depths of 2500 m (common for mid-ocean ridges) the amplitude recovery for the 40-km anomaly is 70% (submarine) and 61% (aircraft) and for the 20-km anomaly, 48% (submarine) and 38% (aircraft).

Two types of noise expected in the airborne signal can impact the anomaly amplitudes. First, motion-induced noise will occasionally superimpose oscillations of a few milliGals on the signal. If the noise is superimposed upon a peak or trough, anomaly amplitude could be erroneously increased. Second, the low-pass filter can distort the anomalies. If an anomaly contains shorter-wavelength information than the filter cutoff, the filter will only pass the longer-wavelength component which can add or subtract anomaly amplitude.

ERS altimeter data are not point measurements of gravity (see section 3.2) but are actually measurements of sea surface height (or slope) distributed over an effective altimeter footprint of 5–10 km or more. As a result, some attenuation of high spatial frequency gravity signal occurs out to wavelengths as long as 50 km or more due to spectral leakage [*Sandwell and Smith*, 1997].

Comparison with the submarine data indicates that ERS 1998 seems to contain more shorter-wavelength signal than the airborne data. Small features in the submarine data are evident in the ERS field but are lost by the airborne filtering and/or upward continuation effects. This conclusion is further supported by the spectral comparison of the ERS field with the GSC ice surface data, where the power in the ERS and the GSC data are essentially equivalent down to ~23 km.

Another issue highlighted by the nearest-neighbor comparison in the Chukchi Borderland region is the difference in level between the two data sets. The nearest-neighbor comparison suggests that both a bias and a tilt exist between the data sets. A bias and/or tilt can be introduced into the airborne measurement by several means. The gravity tie relates the relative gravimeter measurement with an absolute gravity measurement at a bench mark, and, if incorrect, will introduce a bias. Barrow, Alaska, was the airport used for the 1995, 1996, and 1997 surveys. Although the actual benchmark was never exactly found, several land gravity measurements were taken around its reported location. All of these measurements were within 0.1 mGal of each other, and this value was used for the tie.

A tilt and/or bias can also be introduced through scale factor errors, an improperly leveled platform, or through the least squares leveling technique. An incorrect spring tension scale factor will cause an error to scale with an increase of the spring tension reading, as happens as normal gravity increases with latitude and as the Eötvös correction increases. Incorrect scale factors and drift in the zero reading in the horizontal accelerometers can add a bias through an erroneous offlevel correction. A platform poorly adjusted or with hardware problems can also result in a reading that is too low or too high. Steady state horizontal accelerations associated with maintaining a given track heading can change the mean level. The least squares leveling technique can "tilt" the survey. These issues were all addressed so as to reduce or remove their effects. Conditions of platform components are closely monitored, and the level of the platform is checked before and after each flight. Horizontal accelerometer scale factors are calibrated in the laboratory via tilt tests, and the zero reading of each accelerometer is noted before and after each flight and corrected during processing. The off-level correction compensates for the effects of steady state horizontal accelerations. Any error in the spring tension scale factor is demonstrated by systematic differences in intersection errors as much as 3–5 mGal along lines flown east and those flown west as a result of the nearly 900 mGal difference in the Eötvös correction. In both surveys the spring tension scale factor was adjusted to minimize these differences. To prevent the least squares leveling program from tilting the survey, we select all intersections where the error is <2 mGal, calculate the averaged value at each of these intersections, and use these values as constraints in the procedure. For the 1997 survey the leveling procedure adjusted the overall level of the survey by ~0.5 mGal.

Long-wavelength errors in the ERS gravity field would require (1) substantial errors in the long-wavelength ($\lambda > 2000$ km) in JGM-3S [*Nerem*, 1994; *Tapley et al*., 1996] satellite-tracking gravity field used in the remove-restore procedure for ERS gravity computation [*Laxon and McAdoo*, 1998]; (2) systematic errors in the ERS orbits; (3) unspecified limitations in the gravity computation algorithms or the flat Earth assumption in the transform; (4) the uncertain effects of the lack of detailed surface gravity north of 82°N as far field input in the geodetic transformation computations of ERS gravity, or (5) the mapping of steady state ocean currents or regional changes in ice freeboard into the gravity field. Large errors in requirement 1 or 2 have not been identified and seem unlikely. Errors resulting from requirement 3 have not yet been identified. For requirement 4 the lack of data north of 82°N is thought to only create an edge effect that is mitigated by terminating the field at 81.5°N. We found no systematic increase in difference between the ERS and airborne gravity fields as the northern limit of the ERS field was approached that would indicate such a problem. A final concern is the quality of the NIMA 30-min point data along the Siberian margin, which constitute a boundary condition along one half of the map. The original Russian data are Bouguer anomalies provided to NIMA without any information as to how the Bouguer corrections were originally made. Free-air values are approximated by guessing densities and type of Bouguer strategy used and "backing out" the Bouguer correction. The distance to the Siberian margin is thought to make any effects negligible at the Chukchi Borderland region. With respect to requirement 5, dynamic sea surface topography from steady state features (such as boundary currents) would translate into shorter-wavelength gravity features instead of imposing a bias, and any such effects are geographically distant from the Chukchi region.

Without additional data in the Chukchi Borderland for comparison, it is difficult to know which, if either, data set contains the preponderance of the leveling error, and thus insufficient

information exists to constrain its cause. Leveling issues between data sets are a particular problem in the Arctic because of the remoteness of the bench marks and the sometimes lack of agreement of the value at the bench marks (R. Salmon, NIMA, personal communication, 1999). The level differences between Arctic gravity data sets remain an issue to be further investigated.

5.2. Implications for the Arctic Gravity Project

Both the NRL airborne gravity data and the ERS 1998 field provide coherent two-dimensional data sets with internal consistency and uniformity of data characteristics over a broad geographic region. Both data sets are extremely well geolocated. Moreover, this study demonstrates that the ERS 1998 gravity field compares favorably with the best open ocean altimetric marine gravity field in terms of accuracy (rms difference) and resolution (coherence). Previous comparisons between the Scripps/NOAA V7.2 field and shipboard gravity measurements yielded rms differences of 3.1–8.7 mGal [*Marks*, 1996] and 2.65–6.44 mGal, with a mean rms difference of 4.21 [*Yale and Sandwell*, 1999]. In a recent test to further reduce altimeter noise, a comparison of stacked open ocean ERS-1 and -2, Geosat, and TOPEX profiles with shipboard data demonstrated an rms difference of 2.67–5.41 mGal [*Yale and Sandwell*, 1999]. Coherence at the 0.5 level between the V7.2 field and shipboard data range from wavelengths of 23–30 km [*Marks*, 1996], 26 km (V7.2) and 24 km (stacked profiles) [*Yale and Sandwell*, 1999].

In regions of the Arctic Ocean having a smooth gravity field such as the Beaufort Sea, the accuracy of the ERS 1998 gravity field (2.57–3.11 mGal) appears as good as or better than that of the V7.2 field south of the Arctic. The rms differences between ERS 1998 and airborne data in the high-amplitude Chukchi Borderland region (3.63–8.32 mGal) fall within the range of the previous comparisons. In regions of the Arctic Ocean having a rough or rugose gravity field, such as the Chukchi Borderland, the fine-scale limit of resolution of the ERS gravity field is ~19 km, whereas in the regions of smooth gravity this resolution limit falls off to 30–40 km wavelength owing to a weak signal at high spatial frequencies.

The limitations of the airborne and ERS data sets will have the following impact upon the users of the ArcGP map:

1. The resolution limit of 19 km (full wavelength) ensures that the gravity anomalies of medium- and large-scale tectonic features are preserved. This resolution is useful for identifying primary structures and tectonic fabric, such as in basin-wide investigations of tectonic history. However, this map will not preserve finer-scale geologic features. In this case it could function as a reconnaissance map for planning higher-resolution studies.

2. Differences in the short-wavelength anomaly amplitudes between the airborne and the ERS 1998 data will most likely be averaged out by the data compilation process in areas of data overlap. More significant is the overall underestimation of the short-wavelength gravity anomalies by both data sets. End users of the ArcGP map should be aware that anomaly amplitude underestimates over fine-scale tectonic features such as the Northwind Ridge (Figure 8, 205°E), would be a source of errors in gravity modeling.

3. Long-wavelength differences between the data sets are of special concern for combining these data in the ArcGP compilation. These data sets will require tying to other data to correct any long-wavelength problems. Any long-wavelength errors that remain in the final version can significantly impact inversions, such as for depth to Moho, and create large errors in any calculated gravimetric geoid. If properly corrected, the end user will not be impacted.

Given the above caveats, the ArcGP compilation will provide an unparalleled opportunity for western scientists to view the entire gravity field of the Arctic. This compilation will provide much of the information required to unravel the complex tectonic history of the region. It will be a basis for future Arctic geodetic, geophysical, and oceanographic research.

6. Conclusions

The NRL Arctic airborne gravity field and the ERS 1998 field from ERS-1 and -2 altimetry provide important new contributions to Arctic Ocean geoscience. They also provide the foundation for the Arctic Gravity Project compilation, with the airborne data covering two thirds of the deep ocean basins and the ERS 1998 data covering the extensive continental shelves and the Canada Basin. This study highlights the complementary strengths of the two gravity fields. The ERS 1998 field has the advantage of ubiquitous coverage of the ocean south of 81.5°N, a denser sampling of the gravity field, and signal recovery to ~15 km. The airborne data cover a significant portion of the polar hole in the satellite coverage, have lower measurement noise, and recover somewhat higher anomaly amplitudes in the 25–100 km wavelength range. Comparison with ice surface measurements confirms that the Arctic ERS 1998 field is of similar quality to the open-ocean Scripps/NOAA V7.2 marine gravity field. These two data sets should significantly further our understanding of the tectonic evolution of the Arctic Ocean basin.

Acknowledgments. This work was supported under the Crustal Geophysics subelement of the Office of Naval Research Program Element 0601153N, by National Science Foundation grant OPP-9626701 for NRL. We acknowledge the European Space Agency for supplying the ERS waveform (WAP) product. Partial support for DCM was provided by NASA's Solid Earth and Natural Hazards Program (SENH). We thank Walter Roest and D. B. Hearty of the Geological Survey of Canada and Bernard Coakley of Tulane University for sharing their gravity data with us for this comparison. Bernie Coakley and three anonymous reviewers provided helpful reviews of this paper.

References

Andersen, O. B., and P. Knudsen, Global marine gravity field from the ERS-1 and GEOSAT geodetic mission altimetry, *J. Geophys. Res.*, *103*, 8129–8137, 1998.

Ball, D. G., J. L. Jarvis, J. M. Brozena, and M. F. Peters, XOMNI user and technical documentation, Nav. Res. Lab., Washington, D.C., 1995.

Brozena, J. M., V. A. Childers, L. C. Kovacs, and L. A. Lawver, New aerogeophysical evidence for the rotational opening of the southern Canada Basin, *Eos Trans. AGU*, *80*(46), Fall Meet. Suppl., F994, 1999.

Childers, V. A., R. E. Bell, and J. M. Brozena, Airborne gravimetry: An investigation of filtering, *Geophysics*, *64*, 61–69, 1999.

Forsberg, R., and S. C. Kenyon, Arctic Gravity Project (abstract), *Eos Trans. AGU*, *80*(46), Fall Meet. Suppl., F992, 1999.

Forsberg, R., A. Olesen, and K. Keller, Airborne gravity survey of the North Greenland Shelf 1998, report, Kort and Matrikelstyrelsen, Copenhagen, 1999.

Forsyth, D. A., M. Argyle, A. Okulitch, and H. P. Trettin, New seismic, magnetic and gravity constraints on the crustal structure of the Lincoln Sea continent-ocean transition, *Can. J. Earth Sci.*, *31*, 905–918, 1994.

Grantz, A., S. D. May, P. T. Taylor, and L. A. Lawver, Canada Basin,

in *The Geology of North America*, vol. L, *The Arctic Ocean Region*, edited by A. Grantz, L. Johnson, and J. F. Sweeney, pp. 379–402. Geol. Soc. of Am., Boulder, Colo., 1990.

Grantz, A., D. L. Clark, R. L. Phillips, and S. P. Srivastava, Phanerozoic stratigraphy of Northwind Ridge, magnetic anomalies in the Canada basin, and the geometry and timing of rifting in the Amerasia basin, Arctic Ocean, *Geol. Soc. Am. Bull.*, *110*, 801–820, 1998.

Hall, J. K., Chukchi Borderland, in *The Geology of North America*, vol. L, *The Arctic Ocean Region*, edited by A. Grantz, L. Johnson, and J. F. Sweeney, pp. 337–350, Geol. Soc. of Am., Boulder, Colo., 1990.

Harlan, R. B., Eötvös corrections for airborne gravimetry, *J. Geophys. Res.*, *73*, 4675–4679, 1968.

Johnson, G. L., A. Grantz, and J. R. Weber, Bathymetry and physiography, in *The Geology of North America*, vol. L, *The Arctic Ocean Region*, edited by A. Grantz, L. Johnson, and J. F. Sweeney, pp. 63–78, Geol. Soc. of Am., Boulder, Colo., 1990.

Lane, L. S., Canada Basin, Arctic Ocean: Evidence against a rotational origin, *Tectonics*, *16*, 363–387, 1997.

Lawver, L. A., and C. R. Scotese, A review of tectonic models for the evolution of the Canada Basin, in *The Geology of North America*, vol. L, *The Arctic Ocean Region*, edited by A. Grantz, L. Johnson, and J. F. Sweeney, pp. 593–618, Geol. Soc. of Am., Boulder, Colo., 1990.

Laxon, S. W., Sea ice altimeter processing scheme at the EODC, *Int. J. Remote Sens.*, *15*(4), 915–924, 1994.

Laxon, S. W., and D. C. McAdoo, Arctic Ocean gravity field derived from ERS-1 satellite altimetry, *Science*, *265*, 621–624, 1994.

Laxon, S. W., and D. C. McAdoo, Polar marine gravity fields from ERS-1, in *Third ERS Symposium on Space at the Service of Our Environment*, Florence, Italy, *Eur. Space Agency Spec. Publ.*, *SP-414*, 1547–1552, 1997.

Laxon, S. W., and D. C. McAdoo, Satellites provide new insights into polar geophysics, *Eos Trans. AGU*, *79*(6), 69, 72–73, 1998.

Lemoine, F. G., et al., The development of the Joint NASA GSFC and the National Imagery and Mapping Agency (NIMA) Joint Geopotential Model EGM96, *Rep. 17* (*1998-206861*), NASA Goddard Space Flight Cent., Greenbelt, Md., 1998.

Marks, K. M., Resolution of the Scripps/NOAA marine gravity field from satellite altimetry, *Geophys. Res. Lett.*, *23*, 2069–2072, 1996.

McAdoo, D. M., and K. M. Marks, Gravity fields of the southern ocean from Geosat data, *J. Geophys. Res.*, *97*, 3247–3260, 1992.

Nerem, R. S., Gravity model development for TOPEX/Poseidon: Joint Gravity Model 1 and 2, *J. Geophys. Res.*, *99*, 24,421–24,447, 1994.

Peters, M. F., and J. M. Brozena, Constraint criteria for adjustment of potential field surveys, *Geophysics*, *53*, 1601–1604, 1988.

Peters, M. F., and J. M. Brozena, Methods to improve existing shipboard gravimeters for airborne gravimetry, paper presented at International Symposium on Kinematic Systems in Geodesy, Geomatics, and Navigation, Int. Union of Geod. and Geophys., Boulder, Colo., 1995.

Pyle, T. E., M. Ledbetter, B. Coakley, and D. Chayes, Arctic Ocean Science, *Sea Technol.*, *39*, 10–15, 1997.

Sandwell, D. T., and W. H. F. Smith, Marine gravity anomaly from Geosat and ERS-1 satellite altimetry, *J. Geophys. Res.*, *102*, 10,039–10,054, 1997.

Smith, W. H. F., and P. Wessel, Gridding with continuous curvature splines in tension, *Geophysics*, *55*, 293–305, 1990.

Sobczak, L. W., D. B. Hearty, R. Forsberg, Y. Kristoffersen, O. Eldholm, and S. D. May, Gravity from 64°N to the North Pole, in *The Geology of North America*, vol. L, *The Arctic Ocean Region*, edited by A. Grantz, L. Johnson, and J. F. Sweeney, pp. 101–118, Geol. Soc. of Am., Boulder, Colo., 1990.

Taplay, B. D., et al., The Joint Gravity Model 3, *J. Geophys. Res.*, *101*, 28,029–28,049, 1996.

Taylor, P. T., L. C. Kovacs, P. R. Vogt, and G. L. Johnson, Detailed aeromagnetic investigations of the Arctic Basin, 2, *J. Geophys. Res.*, *86*, 6323–6333, 1981.

Telford, W. M., L. P. Geldart, and R. E. Sheriff, *Applied Geophysics*, 770 pp., Cambridge Univ. Press, New York, 1990.

Timmen, L., G. Boedecker, and U. Meyer, Flugzeuggestutzte Vermessung des Erdschwerefeldses Zeitschrift fuer Vermessungswesen, *Jahrgang*, *11*, 378–384, 1998.

Turcotte, D. L., and G. Schubert, *Geodynamics*, 450 pp., John Wiley, New York, 1982.

Vogt, P. R., C. Bernero, L. C. Kovacs, and P. T. Taylor, Structure and plate tectonic evolution of the marine Arctic as revealed by aeromagnetics, *28th International Congress on Geology of Oceans Symposium*, *Oceanol. Acta*, spec. publ., 25–40, 1981.

Vogt, P. R., P. T. Taylor, L. C. Kovacs, and G. L. Johnson, The Canada Basin: Aeromagnetic constraints on structure and evolution, *Tectonophysics*, *89*, 295–336, 1982.

Welch, P. D., The use of the fast Fourier transform for estimation of power spectra: A method based on time averaging over short modified periodograms, *IEEE Trans. Audio Electroacoust.*, *AU15*, 70–73, 1967.

Yale, M. M., and D. T. Sandwell, Stacked global satellite gravity profiles, *Geophysics*, *64*, 1748–1755, 1999.

J. M. Brozena and V. A. Childers, Naval Research Laboratory, Code 7421, 4555 Overlook Ave. SW, Washington, DC 20375. (john.brozena@nrl.navy.mil; vicki.childers@nrl.navy.mil)

S. W. Laxon, Mullard Space Science Laboratory, University College London, Dorking, Surrey RH5 6NT, England, UK. (swl@mssl.ucl.ac.uk)

D. C. McAdoo, NOAA, Laboratory for Satellite Altimetry, Silver Spring, MD 20910. (dave@comet.grdl.noaa.gov)

(Received April 24, 2000; revised October 31, 2000;
accepted November 7, 2000.)